Synthesis and X-ray Crystallographic Characterization of p-Diacetylcalix[4]arene

Young Ja Park*, Kwanghyun No, and Jung Mi Shin

Department of Chemistry, Sook Myung Women's University, Seoul 140-742. *Received May 17, 1991*

A simple route is described for the selective functionalization of calixarene at the para positions of phenyl rings. Calix[4]arene tetraacetate 2, obtained from the treatment of calix[4]arene with acetic anhydride, undergoes Fries rearrangement to yield the diametrically para substituted p-diacetylcalix[4]arene 3 in 80% yield. The crystal and molecular strucutre has been determined by X-ray diffraction method. The crystals are orthorhombic, space group $Pna2_1$, with $a=11.121$ (3), $b=10.374$ (3), $c=21.690$ (6) Å and $Z=4$. The structure was solved by direct method and refined by full-matrix least-squares methods to final R of 0.036 for 1795 observed reflections. Each hydroxyl hydrogen atom is disordered over two positions. The macrocycle exists in the cone conformation which is determined by the strong circular intramolecular flip-flop type hydrogen bonds of phenolic OH, while crystal packing effects of the diametrically para-acetyl substituents seem to be responsible for the distortion of the cone conformation.

Introduction

Calixarenes, which are basket-shaped compounds of potential interest for new host molecules or new type of enzyme mimics, have been synthesized in short synthesis. However, obtained calixarenes are constrained to be symmetrically substituted. The multi-step convergent routes give access to differently substituted calix[4]arenes were developed by Gutsche and No[1] and Bohmer *et al*[2]., but the methods are relatively long, tedious and low in yield. The possibility of adapting the short synthesis to the preparation of unsymmetrically functionalized calix[4]arenes is reported by Reinhoudt[3] and our laboratory[4].

In this investigation we exploit the possiblity of adapting Fries rearrangement for the preparation of partially substituted calix[4]arene. Here we report the synthesis of the diametrically substituted p-diacetylcalix[4]arene and its X-ray crystal and molecular structure determination of the empty form.

Synthesis

When calix[4]arene tetraacetate 2[5], obtained in 75% yield by conc sulfuric acid catalyzed reaction of calix[4]arene 1[6] and acetic anhydride, was treated with excess of $AlCl_3$ in nitrobenzene at room temperature, acetyl groups were rearranged to the para positions of calix[4]arene to yield p-acetylcalix[4]arene[7]. When the reaction was proceeded with smaller ammount of $AlCl_3$, partially rearranged products mixture was resulted and extremely difficult to isolate the pure product. When the compound 2 was treated with limited amount (1.5 mole equivalent per carbonyl group) of $AlCl_3$, only two acetyl groups were rearranged and the remaining two acetyl groups were simply cleaved to produce compound 3 in 80% yield. The diametrical introduction of acetyl groups is confirmed by the singlet pattern of the ^{1}H-NMR resonance peak of the methylene bridge protons at 4.00 ppm[5]. The definite structure of compound 3 was confirmed by X-ray crystal structure determination.

X-Ray Structure Analysis

p-Diacetylcalix[4]arene was recrystallized by slow evaporation of a mixture of chloroform and methanol solution. Preliminary X-ray Weissenberg photographies showed that the crystal system is orthorhombic with space group $Pna2_1$. Subsequent X-ray data were collected using a Nonius CAD-4 diffractometer with Mo-Kα graphite-monochromated radiation ($\lambda=0.7107$ Å). Three standard reflections (2,7,7), (2,7,3), (0,0,16) were monitored for intensity and orientation check every one hour. There was no significant loss of intensities throughout data collection. Among the 1981 independent reflections measured, the 1795 reflections with $|F_o|>2\sigma(F_o)$ were used in structure determination. Data were corrected for Lorentz and polarization effects, but the absorptions were ignored. All of the crystal data are summerized in Table 1.

The phase problem was solved by direct method using the program SHELXS-86[8]. The direct method was applied to 329 reflections with $|E|\geq 1.3$. All the carbon and oxygen atoms were located on the E map. The refinement was carried out with least-squares method, using the programs of XTAL[9] and SHELX-76[8]. Four cycles of isotropic block-diagonal least-squares refinements decreased R value to 0.12. And then anisotropic thermal parameters were introduced for the carbon and oxygen atoms. After two cycles of anisotropic refinement, R reduced to 0.08. At this stage the 24 hydrogen atoms were found on the difference Fourier map and remaining hydrogen atoms attached to the hydroxyl groups were located on the successive difference Fourier maps at $R=0.045$. These four hydrogen atoms were disordered over eight positions. Therefore the occupancy factors were assigned to be 0.5. In the final refinement, the positional parameters of all atoms except hydroxyl hydrogen atoms, the anisotropic thermal parameters for the carbon and oxygen atoms and isotropic thermal parameters for the hydrogen atoms were refined. The occupancy factors of the hydroxyl hydrogen atoms were not refined. The final R and R_w values were 0.036 and 0.039, respectively, for the 1795 observed reflections.

The final atomic coordinates and thermal parameters of the non-hydrogen atoms are given in Table 2.

Description of the Structure

Bond distances and angles with their estimated standard

Table 1. Summary of Crystal Data, Intensity Collection and Least-Squares Refinements Statistics

formula	C_{32} O_6 H_{28}
M_w	508.1
space group	$Pna2_1$
a, Å	11.121 (3)
b	10.374 (3)
c	21.690 (6)
Z	4
μ(Mo-Kα), cm^{-1}	0.54
density, g/cm^3	1.35 (calc.)
	1.35 (mea, by flotation in CCl_4 and C_5H_7OH)
radiation	Mo-Kα (graphite monochromator, λ=0.7107 Å)
crystal size, mm	0.8×0.4×0.2
cell-constant determination	20 reflections (26°<2θ<38°)
2θ range, deg.	2-50
scan type	ω-2θ
scan range, deg.	0.5+0.35 tan θ
No. of observed reflections	1795 $\mid F_o \mid < 2\sigma(F_o)$
R, R_w	0.036, 0.039
w	$1.36/\sigma(F_o)+0.0006(F_o)^2$
ΔF electron density, $e/Å^3$	max. 0.16; min. −0.21
diffractometer	Enraf-Nonius CAD-4

deviations are listed in Table 3. These values are normal as expected for the type of bonds involved.

The conformation of the molecule, shown in Figure 1, is mainly determined by the remarkable intramolecular hydrogen bond system. Each hydroxyl hydrogen atom is disordered over two positions favourable to participate in two hydrogen bonds to two adjacent hydroxyl groups. Therefore there are four hydrogen bonds of the type O-H···H-O. In these bonds, oxygen atoms are in the normal O···O distance range, but two statistically half-occupied hydrogen atoms are arranged between them. The fact that the H···H spearation of ~1 Å is so short that the two hydrogen atoms positions are mutually exclusive and to prevent clashing suggests an equilibrium between two states: O-H···O⇄O···H-O. Of the two hydrogen atoms only one is in hydrogen bonding contact at a given time; the other one is flipped out to form a hydrogen bond with an adjacent acceptor group and vice versa. A comparable scheme has been found in β-cyclodextrin·$12H_2O$, and W. Saenger *et al.*[10] coined the term "flip-fiop hydrogen bond" in this system. The hydrogen bond distances and angles are listed in Table 4.

The inclination of the phenyl rings, A to D, with respect to the least-squares plane of methylene carbons are 135.2, 116.3, 131.7 and 112.4° respectively. The relative dihedral angles between two adjacent rings are: A-B=71.8, B-C=70.6, C-D=105.6 and A-D=105.4° whereas that between two opposite rings are: A-C=88.6 and B-D=48.7°.

The "cone" conformation is more or less distorted, as compared with the ideal 4-fold symmetry found for *tert*-butyl calix[4]arene[11]. This is mainly due to the diametrically substituted para acetyl groups of the phenolic rings A and D.

As shown by nearly equal diagonal and angles close to 90°, the methylene carbons form a regular square. Two other quadrangles, however, are not planar: the quadrangle of the O(1) oxygen atoms and that of C(4) carbon atoms. An increase for the distance O(B)-O(D) and a decrease for the other diagonal O(A)-O(C) are observed. This is necessarily accompanied by increasing values for the angles O(B)-O(C)-O(D) and O(D)-O(A)-O(B) and decreasing values for the an-

Table 2. Fractional Atomic Coordinates (×10^4) and Equivalent Isotropic Thermal Parameters for Non-Hydrogen Atoms of p-Diacetylcalix[4]arene*

$$U_{eq} = 1/3 \sum_i \sum_j U_{ij} a_i a_j^* a_i a_j \quad (Å^2)$$

Atom	x	y	z	U_{eq}
C(1A)	10638 (3)	−1300 (3)	3203 (0)	.039
C(2A)	10515 (3)	−2603 (3)	3419 (2)	.046
C(3A)	9622 (3)	−2777 (3)	3871 (1)	.042
C(4A)	8914 (3)	−1810 (3)	4124 (2)	.047
C(5A)	9037 (3)	−571 (3)	3876 (1)	.038
C(6A)	9884 (3)	−281 (3)	3416 (1)	.038
C(7A)	9948 (8)	998 (8)	3139 (3)	.042
C(8A)	8088 (3)	−2128 (3)	4624 (2)	.043
C(9A)	7244 (4)	−1086 (5)	4849 (2)	.064
C(1B)	9887 (2)	1019 (2)	1946 (5)	.038
C(2B)	9332 (7)	1131 (7)	2529 (3)	.041
C(3B)	8036 (7)	1416 (7)	2504 (4)	.044
C(4B)	7462 (3)	1500 (2)	1965 (5)	.046
C(5B)	8092 (8)	1368 (7)	1403 (3)	.040
C(6B)	9272 (7)	1159 (7)	1401 (3)	.037
C(7B)	9959 (9)	1049 (8)	789 (3)	.047
C(1C)	10592 (3)	−1331 (3)	706 (1)	.044
C(2C)	9879 (3)	−345 (3)	506 (1)	.041
C(3C)	9076 (3)	−593 (4)	49 (2)	.047
C(4C)	8961 (3)	−1817 (3)	−197 (1)	.041
C(5C)	9682 (3)	−2843 (4)	28 (2)	.048
C(6C)	10462 (3)	−2566 (3)	496 (1)	.039
C(7C)	11215 (8)	−3680 (7)	797 (4)	.050
C(8C)	8071 (4)	−2121 (4)	−703 (2)	.064
C(9C)	7248 (4)	−1120 (4)	−944 (2)	.057
C(1D)	11143 (2)	−3697 (2)	1974 (4)	.041
C(2D)	10664 (6)	−4105 (6)	1392 (3)	.038
C(3D)	9709 (7)	−4910 (7)	1401 (3)	.049
C(4D)	9200 (3)	−5336 (3)	−1983 (5)	.055
C(5D)	9668 (7)	−4949 (7)	2498 (4)	.053
C(6D)	10680 (6)	−4094 (7)	2514 (3)	.045
C(7D)	11179 (7)	−3685 (7)	3147 (3)	.045
O(1A)	11487 (2)	−1066 (3)	2797 (1)	.052
O(2A)	8003 (3)	−3173 (3)	4835 (1)	.084
O(1B)	11122 (2)	774 (2)	1974 (4)	.048
O(1C)	11510 (2)	−1047 (3)	1145 (1)	.053
O(2C)	8115 (3)	−3221 (3)	−946 (1)	.071
O(1D)	12143 (1)	−2892 (2)	1957 (3)	.052

* Table for anisotropic thermal parameters of the non-hydrogen atoms, coordinates of hydrogen atoms, structure factors are available from the author (YJP).

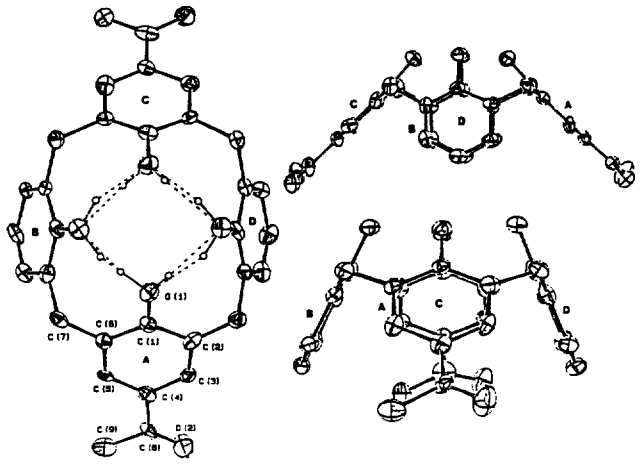

Figure 1. Molecular conformation with atomic numbering of p-Diacetylcalix[4]arene, seen from different directions turned by 90°. Hydrogen bonds are indicated by dotted lines.

Table 3. Bond Distances (Å) and Bond angles(°) for p-Diacetylcalix[4]arene. The e.s.d.'s are in parentheses

	A	B	C	D
C(1)-C(2)	1.437 (4)	1.412 (12)	1.364 (4)	1.434 (10)
C(2)-C(3)	1.406 (5)	1.473 (11)	1.359 (5)	1.351 (10)
C(3)-C(4)	1.390 (5)	1.334 (13)	1.383 (5)	1.453 (12)
C(4)-C(5)	1.400 (4)	1.413 (12)	1.419 (5)	1.295 (13)
C(5)-C(6)	1.404 (4)	1.330 (12)	1.367 (5)	1.433 (10)
C(1)-C(6)	1.427 (4)	1.374 (12)	1.367 (4)	1.346 (10)
C(6)-C(7)	1.458 (9)	1.535 (10)	1.569 (9)	1.540 (9)
C(4)-C(8)	1.459 (6)		1.511 (5)	
C(8)-C(9)	1.513 (6)		1.480 (6)	
C(1)-O(1)	1.313 (3)	1.398 (3)	1.427 (4)	1.391 (3)
C(8)-O(2)	1.180 (4)		1.258 (5)	
C(7D)-C(2A)	1.467 (8)	C(7A)-C(2B)	1.497 (10)	
C(7B)-C(2C)	1.573 (9)	C(7C)-C(2D)	1.495 (11)	

	A	B	C	D
C(3)-C(2)-C(1)	114.3 (3)	114.6 (6)	118.1 (3)	117.5 (6)
C(4)-C(3)-C(2)	125.6 (3)	120.8 (7)	121.1 (3)	120.5 (6)
C(5)-C(4)-C(3)	117.1 (3)	120.9 (5)	120.2 (3)	119.9 (5)
C(5)-C(6)-C(1)	117.8 (3)	120.3 (6)	120.7 (3)	117.9 (6)
C(6)-C(1)-C(2)	122.3 (3)	123.0 (5)	122.4 (3)	122.3 (4)
C(6)-C(5)-C(4)	122.4 (3)	120.6 (6)	117.2 (4)	122.0 (7)
C(7)-C(6)-C(1)	120.8 (4)	119.2 (7)	119.7 (4)	123.7 (6)
C(7)-C(6)-C(5)	121.4 (4)	120.5 (7)	119.5 (4)	118.4 (6)
C(8)-C(4)-C(3)	119.1 (3)		122.2 (3)	
C(8)-C(4)-C(5)	123.8 (3)		177.6 (3)	
C(9)-C(8)-C(4)	117.9 (3)		121.0 (3)	
O(1)-C(1)-C(2)	117.5 (3)	113.9 (8)	118.2 (3)	116.8 (6)
O(1)-C(1)-C(6)	120.2 (3)	123.1 (8)	119.3 (3)	120.8 (7)
O(2)-C(8)-C(4)	123.1 (3)		117.9 (4)	
O(2)-C(8)-C(9)	118.8 (4)		120.8 (4)	
	C(2B)-C(7A)-C(6A)	115.2 (6)		
	C(2C)-C(7B)-C(6B)	112.1 (6)		
	C(2D)-C(7C)-C(6C)	110.9 (6)		
	C(2A)-C(7D)-C(6D)	112.8 (6)		
C(1A)-C(2A)-C(7D)	122.7 (4)	C(3A)-C(2A)-C(7D)	122.5 (4)	
C(1B)-C(2B)-C(7A)	125.8 (7)	C(3B)-C(2B)-C(7A)	119.9 (7)	
C(1C)-C(2C)-C(7B)	122.2 (4)	C(3C)-C(2C)-C(7B)	119.7 (4)	
C(1D)-C(2D)-C(7C)	121.3 (6)	C(3D)-C(2D)-C(7C)	121.1 (6)	

Table 4. Intramolecular Hydrogen Bonds in p-Diacetylcalix[4]arene

D H A	D-H	H···A	D···A	D-H···A
O(1B)-H(O2B)···O(1A)	0.98 Å	1.70 Å	2.645 (7) Å	164°
O(1D)-H(O2D)···O(1A)	0.96	1.85	2.727 (5)	152
O(1A)-H(O2A)···O(1B)	0.99	1.67	2.645 (7)	169
O(1C)-H(O2C)···O(1B)	0.92	1.73	2.644 (7)	174
O(1B)-H(O1B)···O(1C)	0.94	1.79	2.644 (7)	151
O(1D)-H(O1D)···O(1C)	0.99	1.75	2.694 (5)	160
O(1A)-H(O1A)···O(1D)	0.72	2.01	2.727 (5)	173
O(1C)-H(O1C)···O(1D)	0.64	2.06	2.694 (5)	171

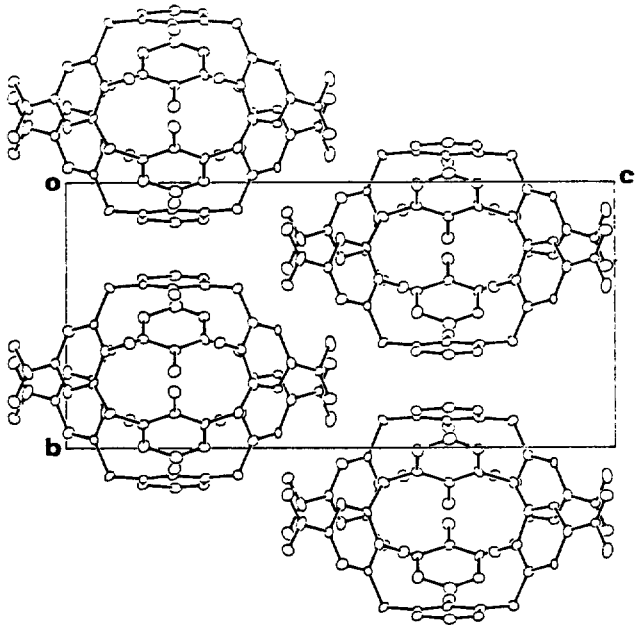

Figure 2. Molecular packing in p-Diacetylcalix[4]arene viewed down the *a*-axis.

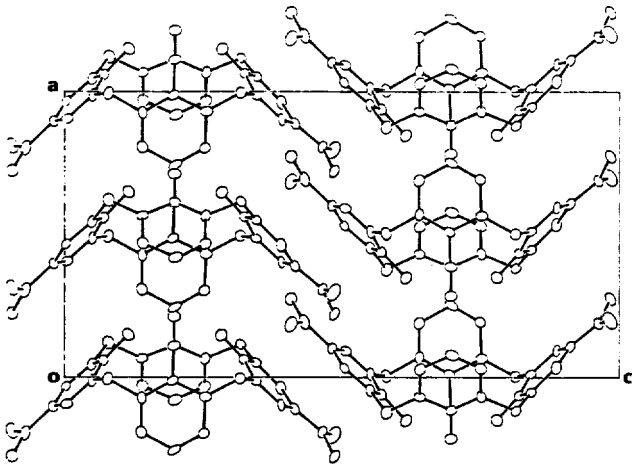

Figure 3. The crystal structure of p-Diacetylcalix[4]arene in projection down the *b*-axis.

Table 5. Torsion Angles(°) for The 16-Membered Macrocyclic Ring in p-Diacetylcalix[4]arene

C(2A)-C(1A)-C(6A)-C(7A)	−173.4 (6)
C(1A)-C(6A)-C(7A)-C(2B)	77.6 (6)
C(6A)-C(7A)-C(2B)-C(1B)	−95.2 (9)
C(7A)-C(2B)-C(1B)-C(6B)	−179.6 (11)
C(2B)-C(1B)-C(6B)-C(7B)	178.6 (11)
C(1B)-C(6B)-C(7B)-C(2C)	95.9 (8)
C(6B)-C(7B)-C(2C)-C(1C)	−80.4 (6)
C(7B)-C(2C)-C(1C)-C(6C)	174.8 (6)
C(2C)-C(1C)-C(6C)-C(7C)	−173.3 (5)
C(1C)-C(6C)-C(7C)-C(2D)	79.7 (6)
C(6C)-C(7C)-C(2D)-C(1D)	−101.6 (8)
C(7C)-C(2D)-C(1D)-C(6D)	−178.3 (10)
C(2D)-C(1D)-C(6D)-C(7D)	179.4 (10)
C(1D)-C(6D)-C(7D)-C(2A)	97.0 (8)
C(6D)-C(7D)-C(2A)-C(1A)	−74.5 (6)
C(7D)-C(2A)-C(1A)-C(6A)	172.1 (6)

Table 6. The Shape of the Calixarene in Terms of Quadrangles

	Phenolic O(1) Atoms	Benzylic Methylene Carbons	C(4) atoms
A-B	2.645 Å	5.098 Å	6.026 Å
B-C	2.644	5.100	6.051
C-D	2.694	5.098	5.980
D-A	2.727	5.047	5.920
A-C	3.584	7.165	9.373
B-D	3.969	7.220	7.351
A-B-C	85.3°	89.3°	101.8°
B-C-D	96.1	90.1	75.3
C-D-A	82.7	89.9	103.9
D-A-B	95.2	90.7	75.9

gles O(A)-O(B)-O(C) and O(C)-O(D)-O(A). Just the opposite deformation of the ideal regular square is observed for the C(4) carbon atoms. The rings B and D pulled into the cavity, and consequently, to keep bond distances and bond angles close to usual values. The rings A and C forced out of the cavity, which can be seen easily from Figure 1.

The C(8A)-C(8C) distance of 11.554 Å is long, therefore intramolecular steric effects of the para-acetyl groups are quite negligible. However the para-acetyl groups are rather important in determining the cone conformation in respect of crystal packing effects.

The crystal structure is shown in Figure 2 and 3. The acetyl group of A ring is packed with that of ring C of the molecule which is symmetrically related by a glide plane perpendicular to the *a* axis. The acetyl groups (see Figure 3) are arranged between the molecules so that the methyl group, $C(9)H_3$, points towards carbonyl O(2) with contacts $CH_3\cdots O$ compatible with the sum of the van der Waals radii. Therefore the rings A and C are strongly forced out of the cavity. It seems that this interaction could be resposible for the distortion of the cone conformation. The B rings of the molecules are packed with D rings of *a* glide plane symmetry related molecules. The intermolecular distances are listed in Table 7.

Table 7. Intermolecular Distances Less Than 3.6 Å

C(5A) --- O(2C)	3.439	a /	1	0	0
C(9A) --- O(2C)	3.460	a /	1	0	0
O(2A) --- C(3C)	3.445	a /	1	−1	0
O(2A) --- C(9C)	3.505	a /	1	−1	0
C(4B) --- O(1B)	3.197	b /	−1	0	0
C(4B) --- C(1D)	3.257	b /	−1	0	0
C(4B) --- C(2D)	3.424	b /	−1	−1	0
C(4B) --- C(6D)	3.403	b /	−1	−1	0
O(1B) --- C(4D)	3.453	b /	0	−1	1
C(5B) --- C(2D)	3.578	b /	−1	−1	0

Symmetry Code: a: $0.5-x$, $0.5+y$, $0.5+z$; b: $0.5+x$, $0.5-y$, z 1 0 −1; translated 1 unit cell along *a*, 0 unit cell along *b*, and −1 unit cell along c.

The results of this study suggest that the distortion of a cone conformation is not sufficient to ensure the intramolecularity since other factors, for instance crystal packing effects, could become predominant.

Experimental

IR spectra were obtained by using a Shimazu IR-435 spectrophotometer, and ^{1}H-NMR spectra were recorded on Varian EM-360 instrument with TMS as internal standard. Melting points were measured in sealed capillary tube using Sybron thermolyne apparatus with polarizing microscope and were not corrected.

25,26,27,28-tetrahydroxycalix[4]arene 1 was prepared in 74% yield by $AlCl_3$-catalized removal of the *tert*-butyl groups from the p-*tert*-butylcalix[4]arene following published procedure[6].

25,26,27,28-tetraacetyloxycalix[4]arene 2 was obtained in 75% yield as colorless crystalline solid as described elsewhere[5].

5,17-Diacetyl-25,26,27,28-tetrahydroxycalix[4]arene 3.

A mixture of 1.00 g (1.69 mmole) of compound 2 and 1.40 g (1.5 mole equivalent per carbonyl group) in 100 m*l* nitrobenzene was stirred for overnight at room temperature, and then added 100 m*l* of water to stop the reaction. After nitrobenzene was removed by steam distillation, the residue was collected by filtration, crushed into powder, washed with water several times, and then dried. Slightly colored solid showed major one spot with three other minor spots on TLC. Colorless powder which was obtained by triturating that solid with acetone was recrystallized from $CHCl_3$/Hexane to give 0.68 g (80%) of crystalline solid: mp. do not melt decomposed up to 350℃; IR (KBr) 3450 cm^{-1} (OH stretching), 1670 (C=O stretching); ^{1}H-NMR ($CDCl_3$) δ 10.3 (s, 4H, OH), 7.87 (s, 4H, ArH), 7.30-6.84 (m, 6H, ArH), 4.00 (br. s, 8H, CH_2), 2.48 (s, 6H, $COCH_3$).

Acknowledgement. This paper was supported (in part) by NON DIRECTED RESEARCH FUND, Korea Research Foundation, 1990.

References

1. K. H. No and C. D. Gutsche, *J. Org. Chem.*, **47**, 2708 (1982).
2. (a) V. Bohmer, F. Marschollek, and L. Zetta, *J. Org. Chem.*, **52**, 3200 (1987); (b) H. Goldman, W. Vogt, E. Paulus, and V. Bohmer, *J. Am. Chem. Soc.*, **110**, 6811 (1988).
3. J.-D. van Loon, A. Arduini, W. Verboom, R. Ungaro, G. J. van Hummel, S. Harkema, and D. N. Reinhoudt, *Tetrahedron Lett.*, **30**, 2681 (1989).
4. K. H. No and M. S. Hong, *Bull. Korean Chem. Soc.*, **11**, 58 (1990) and *J. Chem. Soc. Chem. Commun.*, 572 (1990).
5. C. D. Gutsche, B. Bhawan, J. A. Levine, K. H. No, and L. J. Bauer, *Tetrahedron*, **39**, 409 (1983).
6. C. D. Gutsche and J. A. Levine, *J. Am. Chem. Soc.*, **104**, 2652 (1982).
7. (a) K. H. No, Y. J. Noh, and Y. H. Kim, *Bull. Korean Chem. Soc.*, **7**, 442 (1986); (b) K. H. No and Y. H. Kim, *ibid*, **9**, 52 (1988).
8. G. A. Sheldrick, SHELXS-86 and SHELX-76, A Program for Crystal Structure Determination. Univ. of Cambridge, England (1986, 1976).
9. H. R. Hall and J. M. Stewart, XTAL version 2.2, Univ. of Western Australia and Univ. of Maryland (1987).
10. W. Saenger, Ch. Betzel, B. Hingerty, and G. M. Brown, *Nature*, **296**, 581 (1982).
11. G. D. Andreetti, R. Ungaro, and A. Pochini, *J. Chem. Soc. Chem. Commun.*, 1005 (1979).

The Effect of Minimum Energy Path Curvature on the Dynamic Threshold for Collision-induced Dissociation

Kihyung Song

Department of Chemistry, Korea National University of Education, Chungbuk 363-791.
Received May 28, 1991

In this paper, the question whether the curvature of the minimum energy path can affect the dynamic threshold was tested using the boundary trajectory method developed by Chesnavich and coworkers. For nonreactive system, the MO EXP model potential surface was used with modified equilibrium distance to control the curvature. The results showed that there is no relation between the curvature and the dynamic threshold. In order to study the reactive system, a generalization of the boundary trajectory method was achieved to apply on the nonsymmetric system. We have found no correspondence between the curvature and the dynamic threshold of the system. It was also shown that the fate of the trajectories strongly depends on the shape of potential surface around the turning points along the symmetric stretch line.

Introdution

A series of studies of collision-induced dissociation (CID) has shown that the dynamic threshold for atom-diatom collisions on nonreactive potential surfaces is much larger than the energetic threshold, *i.e.*, the dissociation energy, whereas, for collisions on reactive surfaces, the thresholds nearly coincide[1-4]. An example of the former type is $He+H_2$ collisions and the latter is illustrated by $H+H_2$ collisions.

Bergeron *et al.*[1] suggested that the larger dynamic threshold is typical of nonreactive systems, and is an artifact of collinear model calculations. However, it has been shown that three dimensional systems can also show this behavior[3]. Hence, this behavior appears to be independent of the dimensionality of the system.

Dove *et al.*[3] have argued that the shape of the potential surface is the primary factor governing the behavior of the CID threshold. They noted that when a contour map of the potential energy for an A+BC type reaction is plotted aganinst the A−B and B−C distance, the minimum energy path from the reactant channel tends to curve upward at small A−B distance (toward longer B−C distance) for reactions with an exchange channel (to AB+C), while it curves down (toward shorter B−C distance) for the reactions without an exchange channel. This elongating or shortening of the B−C distance could enhance or reduce, respectively, the dissociation into B+C particles.

In this study, the effect of the shape of the potential surface on the CID threshold for the reaction.

$$H+H_2 \rightarrow H+H+H \quad (1)$$

is tested using model potentials which show both upward and downward curvature for reactive and non-reactive systems. A classical trajectory method for collinear model was used for this study. The effect of incoming particle's mass is also investigated by changing its mass from 1 to 4. The CID boudary method[5-7] is used to determine the dissociative band in the reactant phase space.

In Section II, model potential surfaces used for reactive and nonreactive systems are shown. The method of calculation is explained in Section III, including a brief review of the CID boundary method. Results of this study are presented with discussions in Section IV. A conclusive summary is given in Section V.

Model Potential Surfaces